Wireless Radiation Sensor Network with Directional Radiation Detectors

C. Liu, P.-L. Drouin, G. St-Jean and M. Déziel, D. Waller

***Abstract*—Wireless Radiation Sensor Networks (WRSNs) are promising for military and security applications as they can provide remote detection of sources of radiation with simple, robust radiation detection technologies. This paper shows the results of a combined simulation of wireless networking, and radiation detection with directional gamma-ray detectors. The specific WRSN scenario under study involves a source of radiation being transported through a crossroads. Two different isotopes (^{60}Co and ^{137}Cs) with various activities were simulated to pass through the crossroads at four different speeds (from walking speed to 144 km/hr). A number of different networking and communication protocols were studied. The performance of two algorithms to localize and quantify the radiation sources is presented.**

***Index Terms*—Wireless Radiation Sensor Network, Crossroads, Source Localization, Maximum Likelihood Method, Point of Closest Approach, Zigbee, wireless networking.**

I. Introduction

THIS paper shows the results of a combined simulation of radiation propagation, radiation detection, and wireless network performance. The scenario under study involves a source of radiation being transported through a crossroads, as described in Figure 1. The WRSN is comprised of twelve sensor nodes, one fusion node and a command centre.

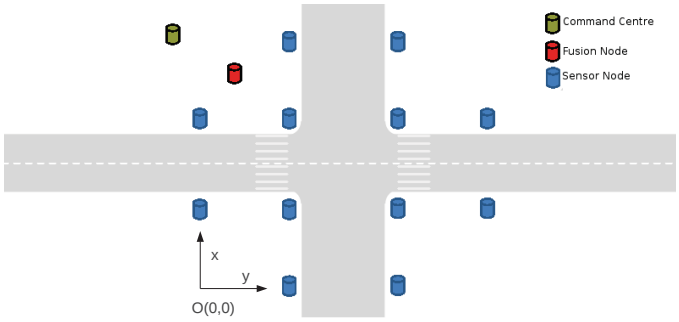

Fig. 1. The crossroads scenario. The fusion node is a computing centre where radiation data from sensor nodes are aggregated and analyzed. The results of threat detection will be informed to first responders at command centre.

II. Directional Radiation Sensors

The directional radiation detectors used in this study are the RadCompass^{TM} detectors built by Bubble Technology Industries [1] at Chalk River, Ontario. The detection units inside RadCompass are four shielded Geiger-Muller (GM) tubes, as shown in Figure 2. The shielding is configured and optimized for rapid source localization. The direction of a source of radiation is determined by comparing the relative count rates between tubes.

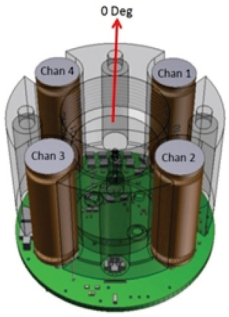

Fig. 2. The RadCompass^{TM} directional radiation detector. An array of shielded GM tubes is used to provide source bearing information.

The response of the detectors was simulated with a simple model based on detailed, experimental measurements of the performance of the RadCompass detectors with a variety of radiological sources in a laboratory setting. The background radiation response has been measured by exposing detectors to different background environments, and has been characterized with statistical models. The models are in turn used for background simulation and detection threshold determination.

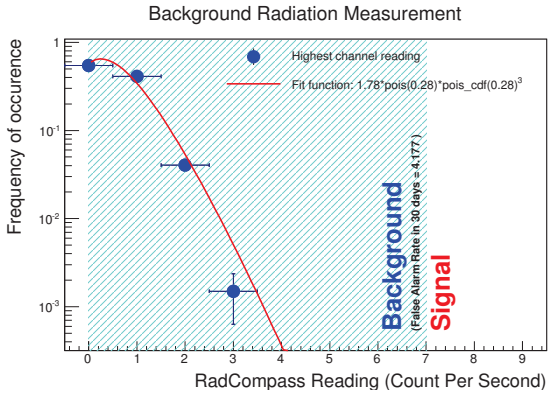

Fig. 3. An example of background radiation measurement with RadCompass. The measurement is fitted with a modified Poisson function which is used to determine the background threshold for a desirable false alarm rate.

Figure 3 gives an example of the background radiation measurement, modelling and threshold determination. In this case, any RadCompass readings less than 7 count per second (cps) are deemed as background. The probability of false alarm is then estimated as low as a few times per month. The false

David Waller, Defence scientist at Defence R&D Canada, Ottawa K1A 0Z4 (David.Waller@drdc-rddc.gc.ca).
Chuanlei Liu and Pierre-Luc Drouin, Calian employee, Ottawa K2K 1Y6.
Guillaume St-Jean and Mathieu Déziel, Engineering Scientists at Communications Research Centre Canada, Ottawa K1A 0Z4.

alarm rate can be dramatically reduced by requiring two side-by-side sensors to simultaneously have a measurement above the threshold.

III. Source Localization Algorithms

Two source localization algorithms have been developed and implemented for use in this work. They are (A) a point-of-closest-approach (PoCA) algorithm, and (B) a maximum log likelihood algorithm (MLL). Both algorithms make use of the TMinuit [2] package in ROOT to carry out the minimization process.

A. The PoCA Method

PoCA is in essence a "Chi-square" method. It formulates a χ^2 based on the distance from a candidate source location to each measured bearing. The χ^2 is calculated and minimized in TMinuit. The iterative process is terminated if a minimum is reached: the candidate source location that minimizes the χ^2 is the PoCA estimate on the location.

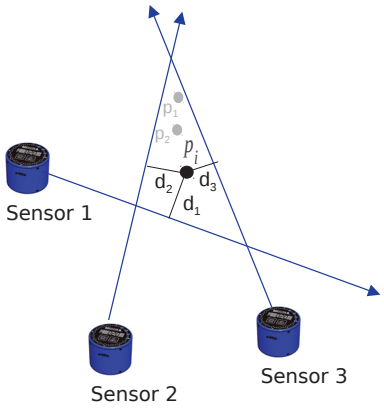

Fig. 4. The PoCA method. At each iteration step i, the distances denoted as d_1, d_2 and d_3 are calculated from the candidate location (p_i) to each bearing vector.

The distance used in χ^2 is calculated based on the geometrical relation between a point (the candidate location) and a line (the source bearing measurement). As Figure 4 describes, at iteration step i, the distances d_1, d_2 and d_3 are calculated for the proposed candidate location p_i with respect to each bearing measurement. Then, χ^2 is calculated by $\chi^2 = \sum_{i=1}^{sensors} \frac{d_i^2}{\sigma^2(d_i)}$. Here the weight $\sigma(d_i)$ is the statistical uncertainty on the distance measurements.

B. The MLL Method

In contrast to PoCA, the MLL method builds a statistical model to describe sensor responses to a source of radiation. The model includes many aspects impacting radiation measurements and relates the sensor measurements to the source activity and location. The aspects included are the inverse square law, air attenuation, sensor shielding effects, detection efficiency and a deadtime correction.

For each measurement, the WRSN sensors provide the numbers of counts which follow Poisson statistics. A joint likelihood function is used to estimate the model parameters of interest for a set of sensor counts. The likelihood function is

$$\mathcal{L} = \prod_{i=1}^{sensors} pois(c_i^{expected}; c_i^{observed}), \qquad (1)$$

where $c_i^{expected}$ is the number of count expected for sensor i, and $c_i^{observed}$ is the actual count observed. The minimum of $-log(\mathcal{L})$ is determined to estimate the source localization.

C. Algorithm Verification

The algorithms have been validated with laboratory experiments, and the results of one such experiments are given in Figure 5. Here a 2x2 array of RadCompass sensors, spaced 1 meter apart, was setup in the laboratory to localize a ^{60}Co source (73.6 MBq). The source is placed at a few locations near the system.

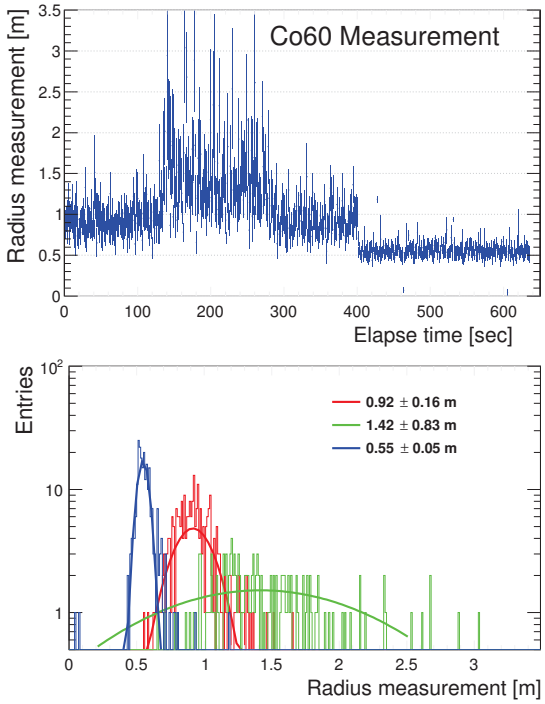

Fig. 5. The top plot displays the distance measurements as time evolves. The distance measurements at each location are fitted with a Gaussian function. The fit results are consistent with the actual distances (0.5, 1.0 and 1.5 meters respectively), as indicated in the bottom plot.

IV. Wireless Network Simulations and Results

The WRSN simulation comprises two parts: the radiation simulation, as described previously in Section II, and a network simulation. The latter studies the network communication aspects by simulating various networking protocols and communications stacks. It determines the latency and probability of data reaching the fusion node.

A. Wireless Network Simulations

The network simulation estimates a number of key metrics that are relevant to military and security applications: (1) the time delay from sensors, (2) the transmission losses (e.g.

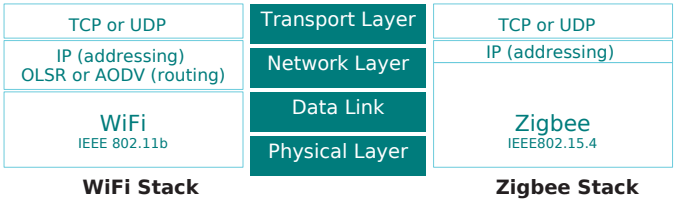

Fig. 6. Simulations of the WiFi and Zigbee communication stacks.

percentage of data packets not reaching the fusion node), and (3) the energy consumption of each node.

The wireless networking was simulated using the QualNet platform [3] from Scalable Network Technologies Inc. The crossroads scenario was modelled, assuming 10 or 20 m separation between adjacent sensor nodes (including the width of the road). Two communication stacks, WiFi and Zigbee, were simulated for WRSN networking. A number of transport, networking (routing) and radio protocols (see Figure 6) were simulated and their performance was studied and compared.

B. Network Simulation Results

Transmission delay: The average transmission delay from sensor nodes to the fusion node varies with the protocol that was employed. The shortest delays occurred with the UDP transport protocol (ranging from 3 ms to 10 ms), while the longest delays occurred with the TCP transport protocol (from seconds up to 40 s). The longer delay with TCP is expected because the mechanism to ensure reliable transport in TCP introduces extra message transmission and overhead. For this metric, UDP is clearly preferable for the crossroads application.

Error rate: UDP has a lower error rate (transmission loss) than TCP. UDP's error rate is typically at a level of a few percent for both stacks, while TCP has about 3 to 10 times larger error rates, depending on the other protocols that are used. For the crossroads scenario, the average error rate is estimated to be about 9% if using Zigbee with UDP. A level of error rate like this one is found to have minimal impact on the final localization performance due to the redundancy of the WRSN sensor nodes.

Energy consumption: The performance of Zigbee and WiFi on energy consumption has been studied. Both stacks were configured to transmit messages at the same rate over the same range. The study shows that Zigbee consumes much less energy than WiFi: approximately 30 times less over the same simulation time period. The power efficiency of Zigbee was achieved by reducing of the packet size and the CPU usage (at idle/sleep states). Zigbee can wake up from the sleep mode in less than 30 ms.

Summary: In general, a WRSN application like the crossroads scenario has a moderate tolerance of transmission loss, but requires small latency for quick detection and fast response. As a result, the UPD transport protocol is an adequate solution. The power consumption of Zigbee is superior to other choices (such as WiFi) as it supports a long term, unattended WRSN deployment.

V. The Crossroads Scenario

A variety of scenarios were simulated in this study. As listed in Table I, two sources of radiation (^{60}Co and ^{137}Cs) with four activities were simulated to pass through a crossroads at four different speeds. The WRSN system was deployed with two topologies to study the impact of sensor spacing.

Source type:	^{60}Co, ^{137}Cs
Activity (Ci):	0.1, 1.0, 10.0, 100.0
Moving speed:	Human walking: 3.6 km/h Low: 36.0 km/h Medium: 72.0 km/h High: 144.0 km/h
System topology:	An array of 12 10m-spacing sensors An array of 12 20m-spacing sensors

TABLE I
The simulated crossroads scenarios.

The radiation responses of detectors were simulated and transmitted through a Zigbee network. The information that reached the fusion node was then aggregated and analyzed by the localization algorithms to estimate the position (and activity) of the radioactive source.

The system coordinates for the crossroads scenario are defined in Figure 1. In this study, a source of radiation is assumed to approach the intersection from the negative-y side and leave it at the positive-y side.

A. Detection and Measurement Thresholds

As previously described, a threshold on count rate (cps$>$7) was determined and it is defined as the *detection* limit. In addition, a tight threshold is used in order to obtain a relatively precise estimation on source measurements. Measurements with ^{60}Co show that the bearing precision level of RadCompass can reach about 1 Octant if its highest cps is equal or greater than 20. This tight threshold (cps $\geq$ 20) is also implemented and is defined as the *measurement* threshold in this study.

B. Detection Limits

For each crossroads scenario, the sensor's detection limit in distance and time is studied. The distance is estimated to be the farthest distance that a sensor can "see" (above the detection threshold) a source. This metric is dependent on the sensor's sensitivity and the source under study. An equivalent representation of the detection distance is the detection "warning" time, that factors in the moving speed of the source.

Similarly, the sensor performance is also examined if the measurement threshold is used. Two metrics in this case are the trackable distance and time.

C. Localization Efficiency And Accuracy

The source localization results are quantified with two metrics: localization efficiency and accuracy. The efficiency is the success rate of a localization algorithm in finding a convergent solution, while accuracy refers to the relative deviation of the estimated source location with respect to the true location.

VI. Crossroads Results and Discussions

An example of the source localization is demonstrated in Figure 7. In this scenario, a ^{60}Co source was simulated passing through a crossroads at a speed of 72.0 km/h. It shows that the source is trackable if within a range of 150 meter from the closest side of the WRSN perimeter. The location is measured more precisely as the source gets closer to the detection system because of increased statistics.

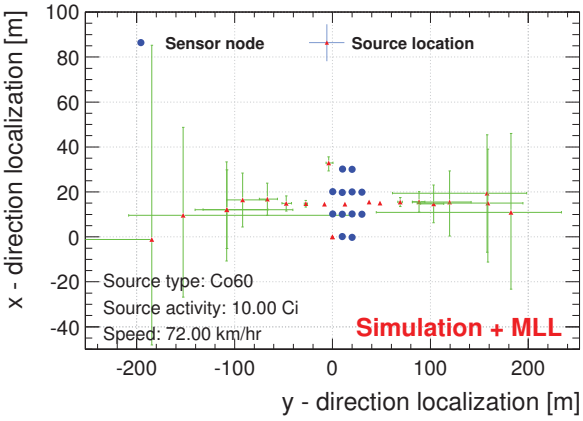

Fig. 7. An example of the localization results as a ^{60}Co source passes through the detection system at a crossroads.

The localization results for ^{60}Co sources varying in activity are presented in Figure 8. The solid coloured histograms in the top plot show the highest count rates of all WRSN sensors. The four plots below it show the localization results as the source activity increases from 0.1 to 100 Ci. As expected, both the detectable and trackable distances increase as the activity increases. The accuracy of the localization also improves as the source is close to or inside the sensor array.

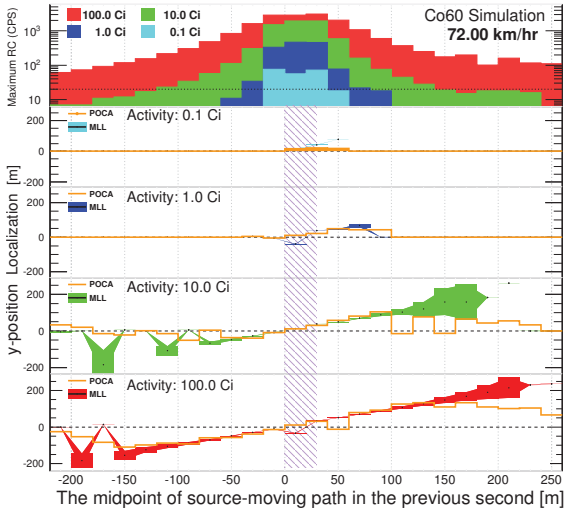

Fig. 8. The sensor count rates and localization results for ^{60}Co sources at different strengths. The hatched region in the middle represents the geographical coverage of the sensor array.

A. Detection Limit Results

Figure 9 shows the detection distance results for various ^{60}Co sources passing through a crossroads at four speeds. As expected, the detection distance (and the trackable distance) tends to follow the inverse square law.

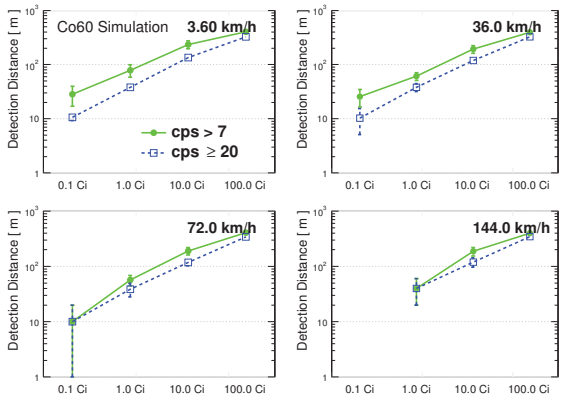

Fig. 9. The detection (cps>7) and measurement (cps≥20) distances for various ^{60}Co sources at four speeds.

The impact of the speed on detection limits is found to be significant when a small source is moving fast. In this case, the source-second (the distance that a source moves in one second) can be used to quantify the relation between speed and detection distance. Taking the 0.1 Ci source as an example, the detection distance is about 20∼30 m at 3.60 km/h. The comparable source-second to this distance requires the source is moving at a speed of 20∼30 m/s (72∼108 km/h). At or above this speed range, the results given in Figure 9 show that the detection either suffers a large uncertainty or ends up with no detection at all.

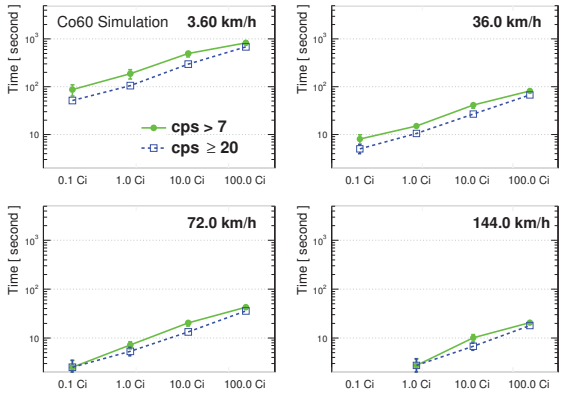

Fig. 10. The detection and measurement times for various ^{60}Co sources at four speeds.

The "warning" time is another measure to characterize and evaluate a WRSN system, especially for moving sources. For the same scenarios discussed above, Figure 10 shows the detection time results. Note the detection time here is estimated at the full range of source propagation, while the detection distance shown in Figure 9 considers only the source

approaching side of crossroads (excluding the sensor coverage area and the departure side). The detection time result provides in-depth information on sensor limit because it additionally explores the speed effect for moving sources.

B. Results On Localization Efficiency And Accuracy

The robustness of the localization algorithms is investigated by studying their efficiency and accuracy. The MLL efficiency results are given in Figure 11 for various ^{60}Co sources passing through a crossroads with a 10 meter spacing WRSN deployment. The low efficiency for 0.1 Ci sources is mainly due to the speed effect, while the other stronger sources are less affected so as to have a higher efficiency overall. In addition, the estimation on these results is subject to the limited counting statistics.

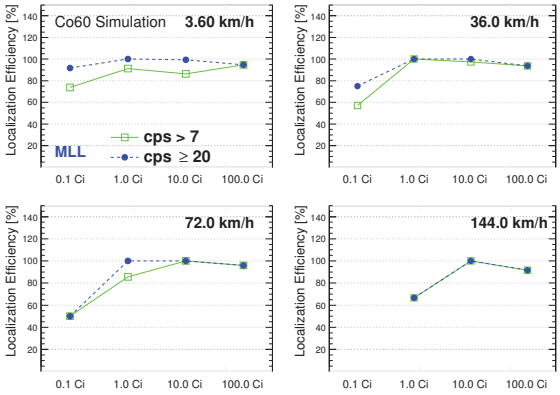

Fig. 11. The localization efficiency with MLL for various ^{60}Co sources as passing through a crossroads with a 10m-spacing WRSN deployment.

The PoCA is expected to produce different results from MLL in terms of localization error. However, the TMinuit algorithm that PoCA uses for minimization is the same as what MLL uses; as such, the success rate (i.e. the detection efficiency) for both algorithms tends to be very similar.

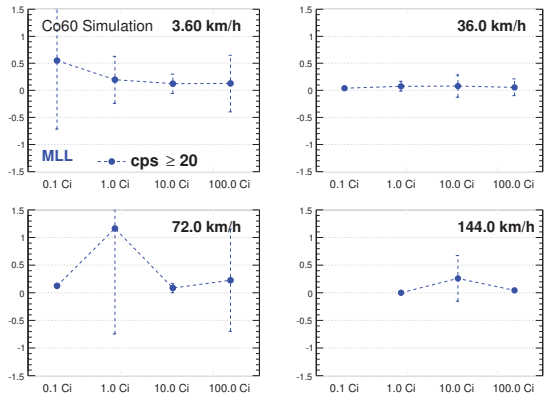

Fig. 12. The localization accuracy with MLL for various ^{60}Co sources passing through a crossroads with a 10m-spacing WRSN deployment.

The localization accuracy was estimated relatively to the true location. It averages all measurements over the detection ranges for each crossroads scenario. The MLL results show $\leq$10% error on source location for most scenarios, as shown in Figure 12. However, it occasionally performs poorly for fast moving small sources. An example of such case is the result of 0.1 Ci source moving at 72.0 km/h. A close look at the results at a second basis can be found in Figure 8. Note the accuracy estimated in this report is a relative value so that it can become large as the true y-position is around zero.

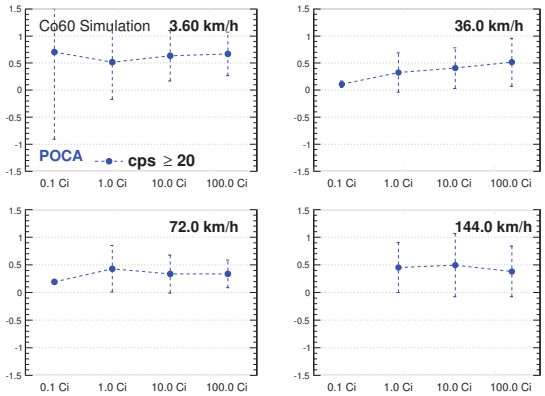

Fig. 13. The localization accuracy with PoCA for various ^{60}Co sources passing through a crossroads with a 10m-spacing WRSN deployment.

By contrast, PoCA performs poorly on accuracy estimation overall. Figure 13 shows its performance for the same scenarios considered in the MLL cases. The accuracy can only reach a level of ~50% for most cases.

A further comparison between MLL and PoCA is made by studying the details of a specific crossroads scenario. The top plot in Figure 14 demonstrates a good linearity of MLL localization, over the full detection/measurement range, between the true y-position and the measured position. A fit on the distribution produces a slope of 1.072, suggesting an overall robust localization performance. The bottom plot displays the fractional difference between the true and measured locations.

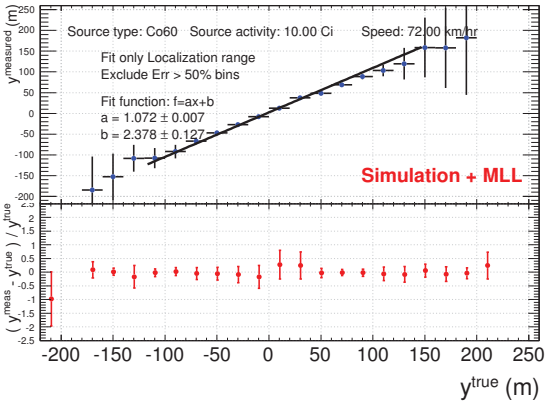

Fig. 14. Detailed MLL localization results for a ^{60}Co scenario.

The PoCA results for the same scenario are shown in Figure 15. The localization range seen in the top plot is smaller than the one with MLL, implying a constrained ability to

localize sources faraway at an acceptable level of accuracy (i.e. less than 50%). As the bottom plot suggests, the localization accuracy using PoCA degrades quickly as distance increases; the algorithm tends to fail to find a solution if the source is beyond a certain range.

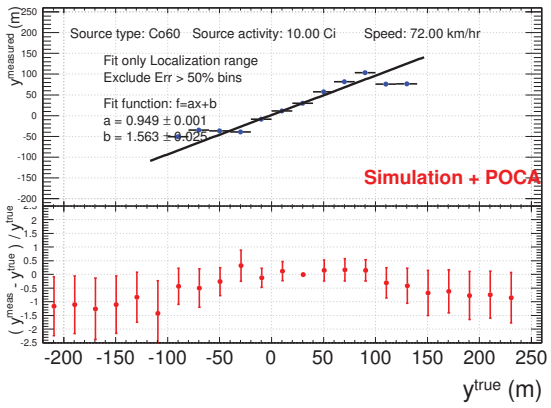

Fig. 15. Detailed PoCA localization results for a ^{60}Co scenario.

C. Other Results

All scenarios have been repeated with ^{137}Cs sources. The detection limit on distance and time is much shorter compared to the same scenario with a ^{60}Co source. The lower sensor count rates for ^{137}Cs due to γ-ray absorption in air is the main reason for this. With regard to the localization performance, no noticeable difference is found between the two source types.

Additionally, all scenarios have been repeated for the other WRSN topology (20m sensor spacing). First, the advantage with a larger spacing is expected and found to increase the detection distance and to help measure fast moving sources. However, the trade-off is the decreased weak source detection capability. Secondly, a large separation between sensors improves the localization performance for both algorithms, especially for the PoCA method, for relatively strong sources.

VII. Summary and Future Work

This paper studies the performance of a WRSN system at crossroads for detecting and localizing moving radiation sources. Various COTS networking technologies are investigated, and their performance is studied and compared. It appears that a Zigbee LAN technology with a UDP transport protocol meets the need of a typical WRSN application. Zigbee with UDP features low energy consumption while achieving an acceptable transmission loss with a short time delay.

A variety of crossroads scenarios were simulated and analyzed. The detection limits are affected largely for fast moving small sources. The spacing between sensors can be adjusted to improve the WRSN performance. Regarding the localization results, MLL produces more robust results than PoCA overall. The localization accuracy improves as the source strength increases.

The technologies and techniques explored, and the results discussed in this study are generic and useful for other WRSN applications. All results suggest that WRSN could be very effective for defence and security applications.

References

[1] Website: www.bubbletech.ca

[2] F. James and M. Roos, *Minuit, A System for Function Minimization and Analysis of the Parameter Errors and Correlations*, Comput. Phys. Commun. 10 (1975) 343-367.

[3] The Qualnet simulator www.scalable-networks.com.